Hydrological Resource Sheds

Thomas E. Croley II[1]; David F. Raikow[2]; Chansheng He[3]; and Joseph F. Atkinson[4]

Abstract: When we consider a location with a material (e.g., water, pollutant, sediment) passing through it, we can ask: "Where did the material come from and how long did it take to reach the location?" We can quantify the answer by defining the areas contributing to this location during various time periods as "resource sheds." Various resource sheds and their source material distributions are rigorously defined and properties derived. For watershed hydrology, we compute resource sheds and their source distributions with a spatially distributed hydrology model by tracing water departing from a "cell" (say 1 km^2) over one time interval, traveling through intermediate cells soil, groundwater, and surface zones, and arriving at the watershed mouth in another time interval. This requires modeling all cells, but only tracing contributions from one at a time. By then combining these simulations for all cell loadings, we construct a map of the contributions over the entire watershed for specific departure and arrival time intervals. We then combine results of several sets of simulations to determine the source distribution for any time period and infer resource sheds from these mappings. We give examples for the Maumee River watershed in northern Ohio, discuss computation reduction, and suggest future extensions to other materials.

DOI: 10.1061/(ASCE)1084-0699(2008)13:9(873)

CE Database subject headings: Hydrology; Runoff; Watersheds; Ohio.

Introduction

Accurately defining the spatial boundary of resource distribution and transport is essential to the understanding and management of resource dispersion over multiple spatial and temporal scales. Since the early twentieth century the *watershed* (land draining into a stream or lake at a given location) has been widely used as a basic unit in hydrologic research [Chow et al. 1988; U.S. Environmental Protection Agency (USEPA) 1995]. A watershed is a hydrologic system that consists of a boundary, an internal structure (drainage areas, vegetation, river channels, lakes, reservoirs, etc.), inputs (water and materials), and outputs (water, services, and pollutants, etc.) (Chow et al. 1988). As a hydrologic system, the boundary, structures, inputs (precipitation, pollutants, etc.), outputs (evapotranspiration, outflow, sediments, etc.), and processes of the watershed change over time and space. Its boundary, for example, is a continuous surface in space enclosing the watershed structure of interest (Chow et al. 1988), ranging from a small tributary (with an area of a few hectares) to a continental river basin (such as the Mississippi River Basin of a few million km^2) along with their attendant surface and subsurface storages. Since the goal of water resources management is to develop and implement policies, processes, technologies, and organizations for understanding, distributing, and improving the movement and characteristics of water resources to meet the multiple needs of human societies and ecosystems in a socially responsible, economically viable, and environmentally sustainable way (He et al. 2005), the watershed is recognized as a natural unit for managing the water resources and associated ecosystem (USEPA 1995; National Research Council 1999; Bruckhorst and Reeve 2006).

Background

Over the years, researchers have extended the watershed concept to water resources and atmospheric studies. Michel (2000), for example, applied the concept of *hydrocommons* (defined as hybrid basins created by linking water sending and receiving basins by conveyance systems such as storage reservoirs and aqueducts) in analyzing the linkages between transbasin water transfers, water quality, and watershed ecosystems. Creation of the hydrocommons removes the natural boundaries of both sending and receiving basins, results in altered hydrology, water quality, ecosystems, economies, and land use patterns in both the sending and receiving watersheds (Michel 2000). Others have used *hydroregion* in understanding the role of regional hydrologic influences in fish species richness (Oswood et al. 2000; Santoul et al. 2004). In atmospheric research, the "air shed" has been used to define the area in which sources of pollutant emissions are located, which are transported and deposited in metropolitan areas or regions, for monitoring and forecasting air quality and implementing management programs such as "ozone action" days (Tullar and Suffet 1975; Chang and Cardelino 2000; Morawska et al. 2002; Ellis et al. 2006).

Similarly, ecologists have sought to spatially delimit otherwise intuitive ecological units such as ecosystems (Cousins 1990). Where changes in ecological conditions are abrupt, such as at the land–water interface of a coast, for example, ecosystem boundaries appear distinct. Yet the phenomenon of ecological subsidy,

[1]Research Hydrologist, Great Lakes Environmental Research Laboratory, 2205 Commonwealth Blvd., Ann Arbor, Michigan 48105-2945. E-mail: tom.croley@noaa.gov

[2]Research Aquatic Ecologist, Environmental Protection Agency, National Exposure Research Laboratory, 26 West Martin Luther King Dr., Cincinnati, OH 45268. E-mail: raikow.david@epamail.epa.gov

[3]Professor, Dept. of Geography, 3234 Wood Hall, Western Michigan Univ., Kalamazoo, MI 49008-5424. E-mail: chansheng.he@wmich.edu

[4]Director, Great Lakes Program, 202 Jarvis Hall, Univ. at Buffalo, Buffalo, NY 14260. E-mail: atkinson@eng.buffalo.edu

Note. Discussion open until February 1, 2009. Separate discussions must be submitted for individual papers. The manuscript for this paper was submitted for review and possible publication on May 1, 2007; approved on November 30, 2007. This paper is part of the ***Journal of Hydrologic Engineering***, Vol. 13, No. 9, September 1, 2008. ©ASCE, ISSN 1084-0699/2008/9-873–885/$25.00.

or donor-controlled supply of resources supporting food webs spatially distinct from source areas, blurs otherwise distinct ecosystem boundaries (Polis et al. 1997). Embracing this common feature of food webs, Power and Rainey (2000) proposed the explicit delineation of ecological subsidy in space through the "resource shed" or "source areas for resources consumed by individuals during their lifetimes." Hence processes, rather than physical landscape features alone, can define geographic areas of ecological relevance to systems under study. Indeed, Power and Rainey (2000) observed that landscape features such as topography, coupled with physical forcing variables, can determine the shape of resource sheds. We generalize the definition of the resource shed to encompass source areas from which materials are derived for an individual, population, or location, over a specified time period. In this definition materials can include nutrients, organic matter, sediments, organism propagules, prey items, or pollutants, i.e., anything transportable by water. Hence, ecologically, a resource shed is a geographic area from which materials originate over a specific time period that subsidize food webs or that are donated to a location at a specific time. Applying this concept, Ben-David et al. (2005) investigate the variable resource sheds created by the movements and behavior of river otters and their impacts on nutrient cycling, changes in productivity and in community structure and function, and landscape heterogeneity of terrestrial communities.

Generalization of the resource shed definition to include pollutants overlaps conceptually with the field of environmental forensics. Primarily concerned with contaminant releases, environmental forensics employs a variety of methods to identify original spill materials (e.g., chemical fingerprinting) and locations (e.g., contaminant source identification) (Murphy and Morrison 2007). While environmental forensics is typically used to reconstruct the history of a contaminant plume (e.g., Bagtzoglou and Atmadja 2005), models simulating the movement of materials have been used to delineate resource shed related areas contributing materials to point locations, such as groundwater "zones of transport" [U.S. Geological Survey (USGS) 2001]. Differences in model components or approaches, however, distinguish previous work from resource sheds as defined here. For example, the presence of pollution sources and the process of biogeochemical transformation during transit are considered within atmospheric "areas of influence" (Habermacher et al. 2007). While environmental forensics has largely focused on contaminants in groundwater and the atmosphere, related studies have been conducted in watersheds. Kalin et al. (2004), for example, produced maps identifying sediment sources by assigning erosion potential values to eight planar elements (catchments) within watersheds.

While the concepts of resource shed and watershed are similar, there are important differences. First, the boundary of a watershed is delineated by elevation and flow direction, following the gravity principle (water flows downhill), and therefore is relatively more stable (e.g., the eight-digit hydrologic unit codes defined by the U.S. Geological Survey for the U.S. watersheds were developed in the 1970s). The boundary of a hydrological resource shed, however, is delineated by the contributing sources of water or other materials to a river or lake (landscape features) during hydrologic events (physical forcing variables). Thus hydrological resource sheds have a more dynamic border, or rather a border relevant to a specific time period during which physical forcing variables operate (e.g., the resource sheds of water or sediments in a watershed change from one storm event to another). Second, the concept of a watershed emphasizes temporal distribution of water and materials within a given space, and the concept of a resource shed focuses on both temporal and spatial distribution of water and materials within a changing space. Third, the watershed concept has been in existence for over 100 years and is understood, accepted, and used worldwide while the resource shed concept is relatively new and not yet well developed. We believe the concept of resource sheds provides a new way of displaying, understanding, and discovering the transport and distribution of water or other materials and has the potential of helping resource managers better track and manage source loadings in a study area.

Expected Uses and Interpretations

We need to compute resource sheds for planning purposes, while interpreting them correctly in terms of scale, because it represents a different perspective than do source material availability maps. Resource shed distribution maps depict source locations for materials contributing to a specific event or period while source material availability maps do not. Resource shed distribution maps combine source availability maps with hydrological transport (surface and subsurface via a distributed hydrology model) to determine the source distribution of an outflow at a location of interest over any time period. Resource sheds allow us to track source areas (just the material actually appearing at a location of interest) in time while source availability maps only show total material availability. For example, consider that every day, we calculate resource sheds for watershed outflow of Atrazine on that day, depicting the source area of this day's Atrazine outflow over the recent past. During an extreme event we could easily answer questions of where it came from and when, essential to resource management decision makers. Another example concerns beach closing warnings for lakes into which a watershed discharges. Currently, measurements of *Escherichia coli (E. coli)* are made in and around beaches to assess the presence of fecal coliform bacteria. (*E. coli* is viewed as an indicator organism). Unfortunately, it takes about 24 h to process the sample and deduce the count, which means that a beach closing, if warranted, occurs 1 day after it is needed. By building resource sheds for microbes, we could not only predict dangerous conditions in near-real time, but also direct land managers to the areas of a watershed where action may be needed. Yet another example concerns harmful algal blooms (HABs) in a lake. Resource sheds over the lake and companion watersheds could show phosphorus and nitrogen source locations relevant to HAB outbreaks and aid in land management. Other examples include sedimentation and delivery of nutrients, pesticides, or contaminants. Multiple resource sheds for several materials may be useful in analyzing yellow perch population fluctuations in the watershed or its outflow or in a receiving lake.

Focus of Paper

Our focus is on resource shed definitions and methodology. Preceding material introduced the concept of resource sheds, showed their relevance to related work, and intimated possible applications. Our intent now is to present rigorous definitions, extensions, and methodologies for resource sheds in general and to illustrate their computation with an example distributed hydrology model. The illustration of resource shed computations should be quite sufficient by using water as the material of interest (instead of sediment, nutrients, or other). The addition of other materials of interest only involves adding appropriate transport and fate equations to the distributed hydrology model but the computation of resource sheds would be the same. However, our example tracing of rainfall from a source area to the location of

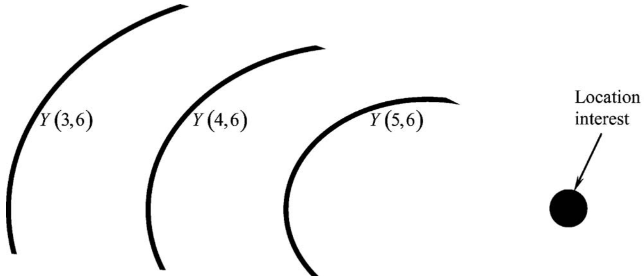

Fig. 1. Example locus (lines) of selected $Y(\tau,t)$

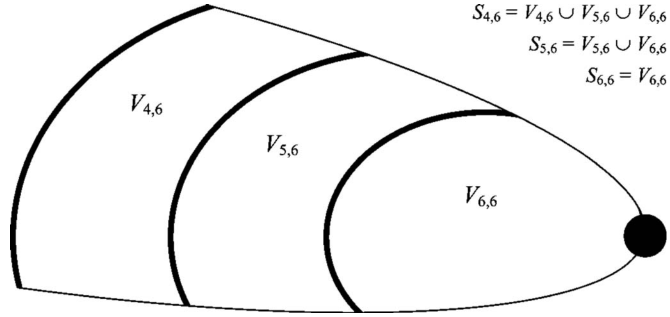

Fig. 2. Example resource sheds for Fig. 1 ($\delta=1$)

interest is a very good proxy for the movement of hydrophilic materials conservative in the short term; these can include acid rain, atmospheric atrazine, carbaryl, and dacthal (Mast et al. 2007). Therefore, our example can be viewed as a contaminant tracing example.

In this paper, we define resource sheds rigorously and propose a set of analysis procedures to determine them. We first describe various resource shed definitions mathematically, providing different views of information that are related, which we then demonstrate. We also describe various resource shed distributions (source density of material of interest over the resource shed) and then demonstrate their relationships. We present methodologies for computing hydrological resource sheds within watersheds through the use of distributed hydrology models and discuss modeling requirements. By using an example distributed hydrology model, we apply the methods to several examples in the Maumee River watershed in northwestern Ohio and discuss computation reduction and near-real-time systems.

Resource Sheds

Definitions

Consider a location with material passing through it (e.g., water, pollutant, sediment). Where did the material come from and how long did it take to reach the location? We can quantify the answer by computing the areas contributing to this location during various time periods. We define such areas as resource sheds. More specifically, let $Y(\tau,t)$ represent the set of all locations where materials departing at time τ arrive at a location of interest at time t, see Fig. 1. [Note in Eqs. (1)–(24), uppercase letters are used exclusively to denote sets, and lowercase letters are used to represent functions or scalars.] Fig. 1 shows $Y(\tau,t)$ as simple lines for a given time (t) for clarity.

We now can define a resource shed a little more rigorously as

$$R(a,b,c,d) = \bigcup_{a\leq\tau<b} \bigcup_{c\leq t<d} Y(\tau,t) \quad (1)$$

where the operator, $\cup$, represents the union of two or more sets. $R(a,b,c,d)$=the set of all locations (resource shed) where materials departing during time interval $[a,b)$ arrive at the location of interest during time interval $[c,d)$. While the definition applies for all time intervals, note that for $a>b$ or $c>d$ or $a>d$, $R=\emptyset$ (the empty set).

For convenience, consider only discrete time in intervals of δ and define

$$V_{i,j} = R((i-1)\delta, i\delta, (j-1)\delta, j\delta) \quad (2)$$

Then $V_{i,j}$=the resource shed where materials departing during the time interval of length δ prior to time i (the ith time interval) arrive at the location of interest during the jth time interval. Also define

$$S_{i,j} = R((i-1)\delta, j\delta, (j-1)\delta, j\delta) \quad (3)$$

$$T_{i,j} = R((i-1)\delta, j\delta, (i-1)\delta, j\delta) \quad (4)$$

where $S_{i,j}$=the resource shed where materials departing during time intervals $i,\ldots,j$ {corresponding to time interval $[(i-1)\delta, j\delta)$} arrive at the location of interest during the jth time interval and $T_{i,j}$=the resource shed where materials departing during time intervals $i,\ldots,j$ arrive at the location of interest also during time intervals $i,\ldots,j$. (For example, a resource shed where atrazine originated and left in the last week of July.) Fig. 2 illustrates $V_{i,j}$ and $S_{i,j}$ corresponding to Fig. 1. Fig. 2 portrays mutually exclusive $V_{i,j}$, $i=j$, $j-1$, $j-2$, ... for clarity. However, all resource shed definitions and derivations herein apply without loss of generality for the general case of overlapping or noncontiguous $V_{i,j}$. Overlapping $V_{i,j}$ for different values of i or j correspond to the case where an area can contribute material over different time intervals to the location of interest. One example is the existence of both surface and subsurface pathways from an area to the location of interest, with different travel times. Another is temporary storage of material (such as sediment) along a flow path: some material from a source area reaches the location of interest quickly while some is delayed. While we depict resource sheds in the definitions sketches of Figs. 1 and 2 as nonintersecting for convenience, the above observation should not be forgotten (that source areas can contribute material at different times to the location of interest). As long as the distributed hydrology model chosen to estimate resource sheds (discussed later) preserves multiple paths and/or travel times, then resource sheds derived from it are fine. Note that

$$S_{i,j} = \bigcup_{m=i,j} V_{m,j} \quad (5)$$

$$T_{i,j} = \bigcup_{m=i,j} S_{i,m} \quad (6)$$

We expect that resource sheds $S_{i,j}$ and $T_{i,j}$ for any time period fully enclose (contain) those for included time periods, for a given location of interest and time. Since

$$\bigcup_{m=i,j} V_{m,j} \subset \bigcup_{m=k,j} V_{m,j}, \quad k\leq i \quad (7)$$

where "$A \subset B$" represents the statement "set A is contained in set B," then by Eq. (5)

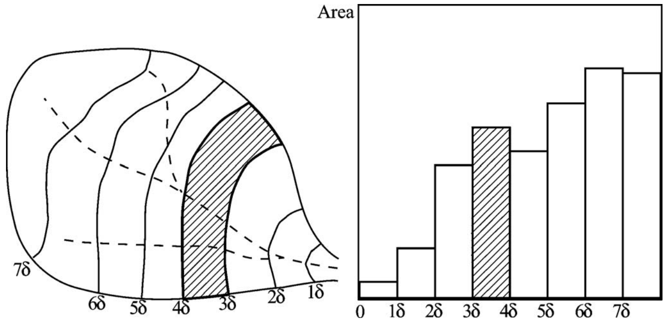

Fig. 3. Isochronal travel time map and resultant time-area histogram

$$S_{i,j} \subset S_{k,j}, \quad k \leqslant i \tag{8}$$

Eqs. (6) and (8) indicate

$$\bigcup_{m=i,j} S_{i,m} \subset \bigcup_{m=i,j} S_{k,m} \subset \bigcup_{m=k,j} S_{k,m}, \quad k \leqslant i \Rightarrow \quad T_{i,j} \subset T_{k,j}, \quad k \leqslant i \tag{9}$$

where "⇒" denotes "implies."

Simple Example Illustration

Note that the classical "travel-time" isochronal map for a watershed (Linsley et al. 1982, p. 280) is an example of our definitions. (It is a simple linear superposition method using steady flows and, since travel times are usually estimated by surface topography, only surface flows are considered in the hydrology.) It is built to estimate a watershed's time-area histogram, which is then used further to estimate the unit hydrograph for a watershed. For example, consider the mouth of a watershed with outflow resulting from the application of a unit depth of water over the entire watershed at time 0. If we determine the travel times from all locations in the watershed to the mouth and plot them, we have the classical hydrological travel time isochronal map shown on the left side of Fig. 3 for an arbitrary watershed. Each isochrone corresponds to $Y(\tau,0)$; for example, the 3δ isochrone represents $Y(-3,0)$. Then, resource sheds ($V_{i,0}$) for water departing during the ith time interval $i=0,-1,-2,\ldots$, and arriving at the watershed mouth during the 0th time interval are those areas with travel times within $[-i\delta,(-i+1)\delta)$; the shaded area in Fig. 3 shows $V_{-3,0}$. By identifying similar resource sheds for other time intervals from the isochronal map, we can build the "time-area" histogram of classical hydrology, shown on the right side of Fig. 3, which can be transformed into an estimate of a unit hydrograph by routing through a hypothetical reservoir. The shaded bar in the time-area histogram corresponds to the shaded resource shed in the isochronal map.

Material Densities

While these definitions refer to the spatial extent of a contributing area, they do not address the differences between parts of a contributing area. Some parts of an area may supply more material to our location of interest than other parts. Define the material's areal density rate of change with departure and arrival times (mass/area/time/time) of material departing location ω at time τ and arriving at the location of interest at time t as

Fig. 4. Example resource shed distribution, $z_{4,6}(\omega)\ \forall\ \omega \in S_{4,6}$, for Fig. 2.

$$h(\omega,\tau,t), \quad \forall\ \omega \in Y(\tau,t) \tag{10}$$

where the expression, "$\forall \omega \in A$," represents the statement "for all ω within set A." Integrating over departure and arrival times, we have the spatial density of material (mass/area), f, at location ω departing during $[a,b)$ and arriving during $[c,d)$

$$f(\omega,a,b,c,d) = \int_a^b \int_c^d h(\omega,\tau,t)dtd\tau, \quad \forall\ \omega \in R(a,b,c,d) \tag{11}$$

Note that for physically relevant situations

$$\begin{aligned} f(\omega,a,b,c,d) &> 0, \quad \forall\ \omega \in R(a,b,c,d) \\ &= 0, \quad \forall\ \omega \notin R(a,b,c,d) \end{aligned} \tag{12}$$

(We omit the distinction in the above equation in the following function definitions, presuming it is understood.) Again for convenience, consider only discrete time intervals of δ and define

$$x_{i,j}(\omega) = f(\omega,(i-1)\delta,i\delta,(j-1)\delta,j\delta), \quad \forall\ \omega \in V_{i,j} \tag{13}$$

Then $x_{i,j}(\omega)$ = the areal density of material at location ω departing during the ith time interval and arriving during the jth time interval. Define

$$z_{i,j}(\omega) = f(\omega,(i-1)\delta,j\delta,(j-1)\delta,j\delta), \quad \forall\ \omega \in S_{i,j} \tag{14}$$

$$w_{i,j}(\omega) = f(\omega,(i-1)\delta,j\delta,(i-1)\delta,j\delta), \quad \forall\ \omega \in T_{i,j} \tag{15}$$

where $z_{i,j}(\omega)$ = the density of material at location ω departing during time intervals $i,\ldots,j$ and arriving during the jth time interval and $w_{i,j}(\omega)$ = the density of material at location ω departing during time intervals $i,\ldots,j$ and arriving also during time intervals $i,\ldots,j$. Fig. 4 illustrates an example resource shed distribution based on Fig. 2; notice there are variations within the resource shed on how much material is contributed. A resource shed boundary can be discerned from a resource shed mapping. From Eq. (12), it corresponds to the border between areas with positive contributions and those with zero contributions. Note that

$$z_{i,j}(\omega) = \sum_{m=i,j} x_{m,j}(\omega), \quad \forall\ \omega \in S_{i,j} \tag{16}$$

$$w_{i,j}(\omega) = \sum_{m=i,j} z_{i,m}(\omega), \quad \forall\ \omega \in T_{i,j} \tag{17}$$

Note that Eqs. (16) and (17) do not represent linear superposition. They follow simply from the definitions of Eqs. (13)–(15). In other words, the material arriving at the location of interest in time interval j from time intervals $i,\ldots,j$ $[z_{i,j}(\omega)]$ is composed of material arriving in time interval j from time interval i plus that from time interval $i+1$, plus that from time interval $i+2,\ldots$, plus that from time interval j. Likewise, the material arriving at the location of interest over time intervals $i,\ldots,j$ that originated over time intervals $i,\ldots,j$ $[w_{i,j}(\omega)]$ is composed of the material arriving in time interval i originating over time intervals $i,\ldots,j$ plus that in time interval $i+1$, plus that in time interval $i+2,\ldots$, plus that in time interval j. In fact, Eqs. (16) and (17) do not represent superpositions of any kind; rather they represent that the total is the sum of it parts.

Similar to resource sheds, we expect resource shed distributions for any time period to enclose (be greater than or equal to) those for included time periods, for a given location of interest and time. Since $x_{i,j}(\omega)$, $z_{i,j}(\omega)$, and $w_{i,j}(\omega)$ are strictly positive within their encompassing resource sheds, then similar to Eqs. (7) and (8), for all ω

$$\sum_{m=i,j} x_{m,j}(\omega) \leqslant \sum_{m=k,j} x_{m,j}(\omega), \quad k \leqslant i \Rightarrow z_{i,j}(\omega) \leqslant z_{k,j}(\omega), \quad k \leqslant i \tag{18}$$

Eqs. (17) and (18) indicate for all ω

$$\sum_{m=i,j} z_{i,m}(\omega) \leqslant \sum_{m=i,j} z_{k,m}(\omega) \leqslant \sum_{m=k,j} z_{k,m}(\omega), \quad k \leqslant i$$
$$\Rightarrow w_{i,j}(\omega) \leqslant w_{k,j}(\omega), \quad k \leqslant i \tag{19}$$

Estimating Resource Sheds

Spatial Integration into Cells

In a watershed, we can compute resource sheds from spatially distributed hydrology models that consider more hydrology than the previous simple example and are not limited to simple superposition. Material placed anywhere in the watershed will appear at the watershed outlet (mouth) over a period of time. We calculate the material appearing at the mouth (our location of interest) at any time, contributed by a specific area. We consider each *cell* c of watershed surface by tracing material departing the cell in time interval i and arriving at the mouth in time interval j, $\bar{x}_{i,j,c}$, where the full watershed hydrology is considered influencing the travel time and surface and subsurface flow paths

$$\bar{x}_{i,j,c} = \int_{A_c} x_{i,j}(\omega)d\omega, \quad \forall A_c \in V_{i,j}$$
$$= \int_{A_c} x_{i,j}(\omega)d\omega, \quad c = 1, \ldots, v_{i,j}/a \tag{20}$$

where A_c=the set of all locations comprising cell c, $v_{i,j}$=the area of $V_{i,j}$, and a=the area of A_c, $c=1,\ldots,v_{i,j}/a$ (all cells have the same area); the units of $\bar{x}_{i,j,c}$ are mass. This requires modeling all cells but tracing contributions from only one at a time. Since it involves no more computation, we simulate material movement from each cell c during time intervals $i,\ldots,j$ to the mouth in time interval j, $\bar{z}_{i,j,c}$, by Eq. (16)

$$\bar{z}_{i,j,c} = \int_{A_c} z_{i,j}(\omega)d\omega = \int_{A_c} \left[\sum_{m=i,j} x_{m,j}(\omega)\right]d\omega, \quad \forall A_c \in S_{i,j}$$
$$= \sum_{m=i,j} \int_{A_c} x_{m,j}(\omega)d\omega = \sum_{m=i,j} \bar{x}_{m,j,c}, \quad \forall A_c \in S_{i,j}$$
$$= \sum_{m=i,j} \bar{x}_{m,j,c}, \quad c = 1, \ldots, s_{i,j}/a \tag{21}$$

where $s_{i,j}$=the area of $S_{i,j}$. Similarly we can combine results of several sets of simulations as in Eq. (17) to determine the source distribution of departing material in the watershed going through the mouth in any specified time period

$$\bar{w}_{i,j,c} = \int_{A_c} w_{i,j}(\omega)d\omega = \int_{A_c} \left[\sum_{m=i,j} z_{i,m}(\omega)\right]d\omega, \quad \forall A_c \in T_{i,j}$$
$$= \sum_{m=i,j} \int_{A_c} z_{i,m}(\omega)d\omega = \sum_{m=i,j} \bar{z}_{i,m,c}, \quad \forall A_c \in T_{i,j}$$
$$= \sum_{m=i,j} \bar{z}_{i,m,c}, \quad c = 1, \ldots, t_{i,j}/a \tag{22}$$

where $t_{i,j}$=the area of $T_{i,j}$. (We can again deduce resource sheds as described previously). Note that Eqs. (21) and (22) use exact spatial integrals with no superposition or linear system assumptions; they use only that an integral of a sum of functions is equal to the sum of the integrals of the functions where all are functions of the same integrative variable (CRC 1969). This is always true regardless of the linear/nonlinear nature of the functions, which is determined by the distributed hydrology model (see the succeeding material).

Material Fractions

We can also calculate relative fractions as well as absolute amounts; they will be useful later as source density estimates. Represent the material fraction arriving in time interval j that departed in time interval i from an area A_c as $p_{i,j,c}$. Represent the material fraction arriving in time interval j that departed during time intervals $i,\ldots,j$ from area A_c as $q_{i,j,c}$. Finally, represent the material fraction arriving during time intervals $i,\ldots,j$ that departed during time intervals $i,\ldots,j$ from area A_c as $u_{i,j,c}$. Note that

$$p_{i,j,c} = \frac{\bar{x}_{i,j,c}}{g_j}, \quad c = 1, \ldots, v_{i,j}/a$$

$$q_{i,j,c} = \frac{\bar{z}_{i,j,c}}{g_j}, \quad c = 1, \ldots, s_{i,j}/a$$

$$u_{i,j,c} = \frac{\bar{w}_{i,j,c}}{\sum_{m=i,j} g_m}, \quad c = 1, \ldots, t_{i,j}/a \tag{23}$$

where g_j is the total material arriving at the location of interest in time interval j. Note that

$$q_{i,j,c} = \frac{1}{g_j}\sum_{m=i,j} \bar{x}_{m,j,c} = \frac{1}{g_j}\sum_{m=i,j} g_j p_{m,j,c} = \sum_{m=i,j} p_{m,j,c}$$

$$u_{i,j,c} = \left[\frac{1}{\sum_{m=i,j} g_m}\right] \sum_{m=i,j} \bar{z}_{i,m,c}$$
$$= \left[\frac{1}{\sum_{m=i,j} g_m}\right] \sum_{m=i,j} g_m q_{i,m,c}$$
$$= \sum_{m=i,j} \gamma_{i,j,m} q_{i,m,c} \quad (24)$$

where $\gamma_{i,j,m} = g_m / \sum_{k=i,j} g_k$, which is the fraction of all material arriving at the location of interest during time intervals $i, \ldots, j$ that arrived in time interval m $(i \leq m \leq j)$.

Hydrology Model

The choice of the distributed hydrology model to use in estimating resource sheds depends upon the requirements (material to be traced, temporal/spatial resolutions required and realistic, and confidence) and facility of use. A classical scale problem in distributed watershed hydrology is resolving contributions to watershed outflow from different source areas from the integrated response hydrograph at the outlet, especially as the spatial scale becomes finely defined. Also, since different combinations of sources could give the same integrated hydrograph, there is also the problem of uniquely identifying source areas from consideration of the hydrograph alone. However, we are not attempting to "work backward" from an observed hydrograph to discern source areas. Instead, by changing our perspective and utilizing information on the spatial distribution of source materials, meteorology, and watershed characteristics, we use much more information than just the integrated hydrograph. For example, we may have observed spatial distributions for topography (elevation, flow direction, slope), soils (surface, upper and lower soil and groundwater zones depths, available water content, permeability, texture, and roughness) and land use as well as spatial–temporal distributions of meteorology, material applications, and land management. Utilizing this information in a distributed hydrology model requires calibration or verification with observations of material transport to achieve confidence in the model application. Thus the model would have to be shown as a good representation of the watershed before it can be used to compute resource sheds. The evaluation of estimated resource sheds requires observation mapping of source material every day and measuring outputs. But, that is no different from standard calibration or validation of the distributed hydrology model that is used in the resource shed estimation.

The distributed hydrology model used to compute resource sheds should be a continuous simulation model. It is used to simulate over a period, prior to the period of interest, long enough to eliminate the effect of initial conditions, and to minimize the presence of untraced flows from earlier times.

Finally, note that superposition is not part of resource shed concepts and definitions. Superposition can only be introduced into resource shed estimates by means of the chosen distributed hydrology model (as it was in the classic time-area histogram example).

Example Maumee River Resource Sheds

Example Distributed Hydrology Model

As an illustration of these resource shed definitions and methods, we chose consideration of water flows only (or considered as a proxy for some hydrophilic conservative contaminants), as stated in the Introduction. We use the Great Lakes Environmental Research Laboratory's (GLERL's) distributed large basin runoff model (DLBRM) to model watershed outflow. While we are adding transport mechanics to it for sediment, nutrients, and microbes and will be calibrating them to field measurements taken over the next 2 years for areal surveys and in-stream measurements, the DLBRM's present form is sufficient to demonstrate the methodology while allowing a few interpretations. The DLBRM represents each "cell" (1 km^2) of a watershed's area as a cascade of moisture storages or "tanks," each modeled as a linear reservoir, where tank outflows are proportional to tank storage, see Fig. 5. Snow melt is limited to snow accumulation and proportional to air temperature each day when temperatures are above freezing and infiltration into the top soil tank is a function of tank saturation (variable area infiltration where zero area corresponds to complete saturation). The model computes potential evapotranspiration from heat available during the day, which is proportional to an exponential function of normalized air temperature, and computes actual evaporation or evapotranspiration for each tank from the potential evapotranspiration and the moisture content of the tank; potential and actual evapotranspiration are therefore noncomplementary, appropriate for small areas. Thus, while tank flows are linear to storage, snowmelt and evapotranspiration are not. Each tank has lateral flows between cells (an upstream flow

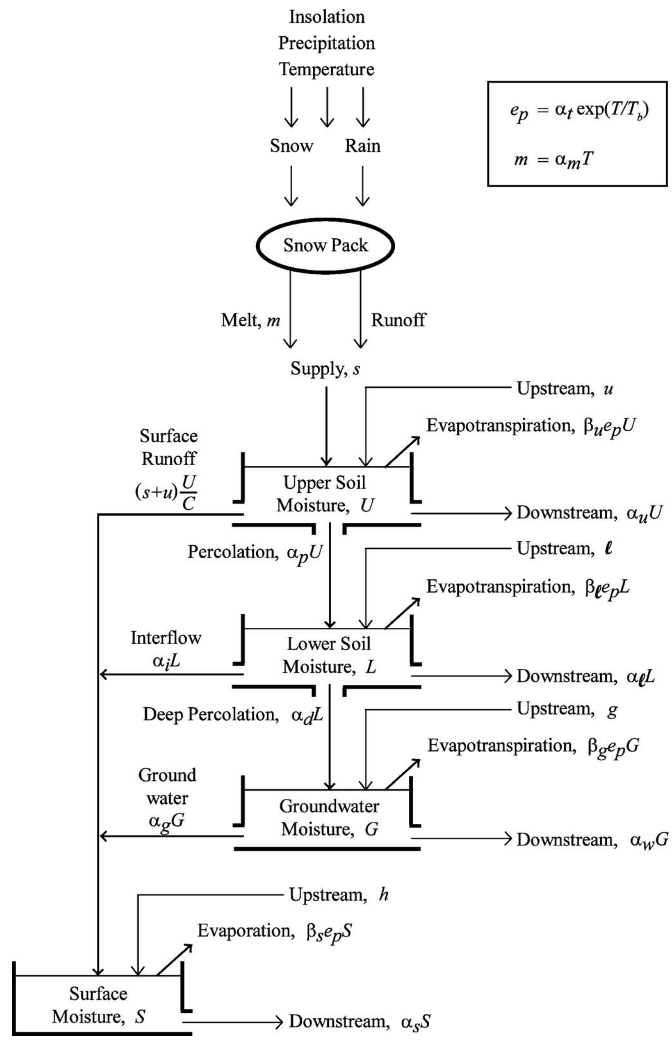

Fig. 5. DLBRM schematic for one cell

into the tank and a downstream flow out of the tank). Thus there are eight lateral flows for all moisture storages (upstream to and downstream from the surface zone, upper soil zone, lower soil zone, and groundwater zone). Each cell's inflow hydrographs must be known before its outflow hydrograph can be modeled and the DLBRM arranges calculations by flow network to assure this. Thus, a cell's entire input hydrographs for the surface zone, upper soil zone, lower soil zone, and groundwater zone are computed for all immediately upstream watershed cells and used as boundary conditions for computation of the cell's output hydrographs. If a cell has more than one set of inflows, all are combined as boundary conditions for the computation. The computations are implemented to minimize the number of pending hydrographs in storage and the time required for them to be in storage. The model uses the same routing network for lateral flows between all surface storages, all upper soil zone storages, all lower soil zone storages, and all groundwater zone storages.

The spatial scale of the model was chosen to allow us to accommodate several scales [soil parameters from a state soil geographic database (STATSGO), topography from the USGS, meteorology from the National Weather Service, land use from a USGS land-cover database, and upcoming erosion parameters from the U.S. Department of Agriculture and upcoming field surveys of manure, nutrient, and atrazine from the Michigan Departments of Environmental Quality and Natural Resources and Ohio Environmental Protection Agency]. We picked a relatively fine resolution only to avoid registration errors and to fairly represent the intersections of various areas defined at different scales. The model works well at the fine scale, but of course the information produced at this scale may be open to interpretation. That is the subject of other studies and was not pursued further here.

As mentioned above, the DLBRM provides a framework for adding erosion and transport models for sediment, nutrients, insecticides, microbes and so forth. As these various components are added, their availability in time must also be considered. For example, consideration of phosphorus as a source material requires knowledge of its application throughout the watershed as well as erosion, sedimentation, water flow, and fate models. Again, since we are only interested here in an illustration of resource shed computations, the DLBRM for water (or a hydrophilic conservative contaminant) as the material of interest should be quite sufficient.

The model also considers many watershed characteristics indirectly. For example, tile drains exist in the Maumee watershed and, while not included directly, are represented in the spatial watershed data sets for land use, permeability, and roughness observations. The same is true for marshy areas.

Hydrology Model Calibration

Since the performance measure for resource shed estimates is simply the goodness of fit of the chosen distributed hydrology model to observed data, it is worthwhile to explain the calibration procedure we used with the DLBRM. For the Maumee application there are 16 model parameters as shown in Fig. 5; they are defined in the Notation section. The heat constant, α_t, is selected to match a long-term heat balance (for given values of the base temperature, T_b, and snowmelt coefficient, α_m) leaving 15 model parameters to be determined in a calibration (C, T_b, α_d, α_i, α_g, α_ℓ, α_m, α_p, α_s, α_u, α_w, β_u, β_ℓ, β_g, and β_s). There are 17,541 cells in the watershed, implying over a quarter million parameters, which is extensively large resulting in very high uncertainty with the selected set or even the inability to calibrate with available data. On the other hand, if each cell has the same set of parameter values so that calibration is possible, then much of the distributed nature of the model is lost. Taking a hybrid approach, we define the 15 parameters as the spatial averages and represent each one's spatial variation with the spatial variation of a selected observation. For example, for the percolation coefficient, $\bar{\alpha}_p$ represents the spatial average with its spatial variation given by $(\alpha_p)_c$; for the upper soil zone capacity, $\bar{C}$ represents the spatial average value and $(C)_c$ represents its spatial variation

$$(\alpha_p)_c = \bar{\alpha}_p b(K_c^U, 80\,\%), \quad c = 1, \ldots, n$$

$$(C)_c = \bar{C} b(C_c^U, 80\,\%), \quad c = 1, \ldots, n \tag{25}$$

where K_c^U = the observed permeability in the upper soil zone in the cth cell, C_c^U = the observed upper soil zone water capacity in the cth cell, n = the number of cells in the watershed, and the spatial distribution function, b, is

$$b(y_c, \varepsilon) = \left(\frac{y_c}{\frac{1}{n}\sum_{j=1}^{n} y_j} - 1 \right) \frac{\varepsilon}{100\%} + 1 \tag{26}$$

where y_c = data value for cell c and ε = fraction of observed range to use (in percent) as the parameter range. Each of the remaining parameters are assigned one of the observed spatial variables (Croley and He 2006) except for the snowmelt and potential evapotranspiration parameters (α_m and T_b, respectively), which are taken as spatially constant, and for the surface and groundwater evapotranspiration coefficients (β_s and β_g, respectively), which are taken as zero. Thus, the 13 spatial average parameter values are found from a calibration using spatial variation defined by relations such as Eq. (25) (Croley and He 2006) for 11 of them. The calibration is made to minimize the root-mean-square error (RMSE) between model and observed daily outflow at the watershed outlet over a calibration period. (Results for different calibration periods are in the next paragraph.) The 13-dimensional parameter space is systematically searched by using gradient search techniques to find the minimum RMSE. See Croley and He (2005, 2006) and Croley et al. (2005) for DLBRM details and Croley (2002) for the earlier lumped-parameter model, which preceded the DLBRM. To speed up calibrations, we preprocess all meteorology for all watershed cells and preload it into computer memory. Finally, as we add other materials (besides water) to our DLBRM for use in later studies, we not only must add transport mechanics to the model, but must gather input spatial observations and output flows for these other materials. We would then compare model outflows of these other materials to the observed and adjust the additional parameters [again finding the spatial average parameter values in a calibration but considering the parameters' spatial variation in a similar fashion to Eq. (25)]. We anticipate adding only one or two additional materials at a time to keep the calibrations simple and building upon added material dynamics as we add yet more materials. For example, we are starting with erosion and sediment transfer and when finished will add phosphorus, which depends on sediment.

Calibration of the Maumee DLBRM for 1950–1964 daily spatial meteorology, topography, land use, soil parameters, and surface roughness and daily outlet runoff produced 0.90 correlation between modeled and observed outflows, 78.5% RMSE as compared to average runoff, 0 bias, and a Nash–Sutcliffe (NS) value of 0.73. Since near-unit values of correlation and the NS statistic and near-zero values of RMSE and bias are sought, the calibration

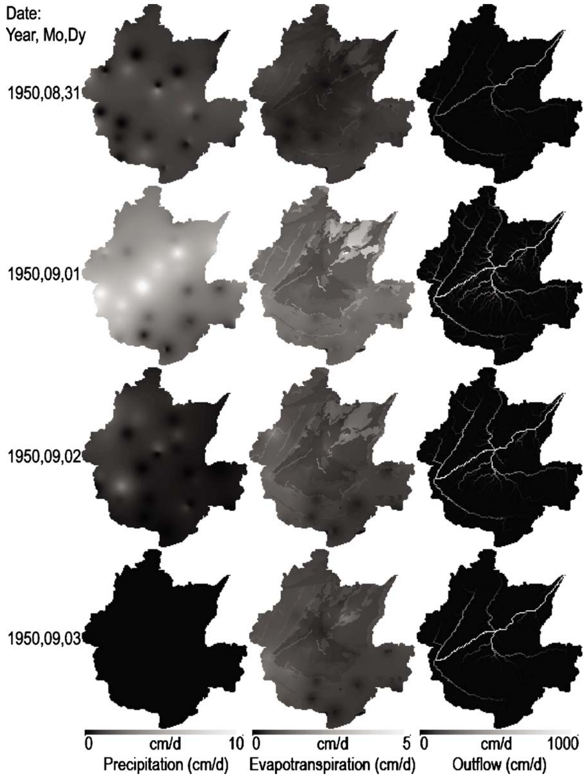

Fig. 6. Maumee river watershed model animation for August 31–September 3, 1950

was judged to be very good. A verification using the 1950–1964 calibrated parameters with 1999–2002 data produced 0.90 correlation, 71.3% RMSE, 2.3% bias, and 0.72 NS; again very good. Finally, a recalibration to 1999–2002 data produced 0.91 correlation, 67.3% RMSE, 6.7% bias, and 0.76 NS, judged the best. We have also used in-stream flow tracers to finely adjust surface flow parameters. The model is being used in other studies in association with Lake Erie prediction of beach closings, harmful algal blooms, yellow perch survivability, and food chain issues.

Example Hydrology Model Output

We built watershed maps showing each simulation day's watershed variables, arranged them in chronological sequence for each variable, and played them as an animation over the simulation period. There is a total of 32 variables (see Fig. 5) and three of these are depicted in Fig. 6 for a 4-day simulation to illustrate the DLBRM's application to the Maumee watershed. Fig. 6 shows example animation frames for the Maumee watershed in northwest Ohio. The watershed outlet is to the northeast; see the right column maps in Fig. 6 showing surface flows. In Fig. 6, a storm peaks on September 1, 1950 and its pattern and intensity are obvious from the first column of pictures in Fig. 6. The figure also shows that evapotranspiration is much higher on September 1 than on other days (see the middle column of pictures) and that surface response is higher too (see the right column of pictures). The surface outflow network is seen as most extensive during the storm peak. The Maumee is a very "flashy" watershed that responds quickly to surface supply. Note that while the spatial structure of the precipitation is revealed in the first column of pictures in Fig. 6, the second column of pictures reveals the spatial structure of the watershed as well as of the precipitation supply. These spatial variations mimic upper soil zone permeability. Likewise, the third column of pictures reveals the spatial structure of the drainage network.

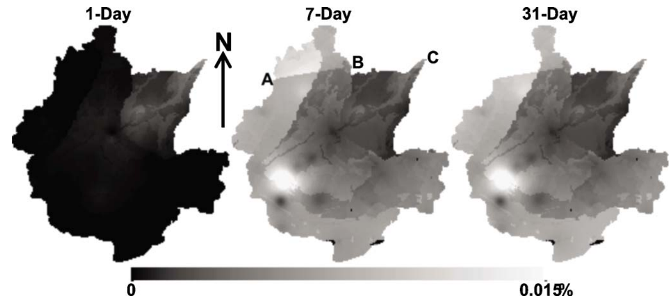

Fig. 7. Maumee resource sheds on January 1, 1950 from prior days of loading: 1-day: $q_{\text{January 1,1950,January 1,1950},c}$ $c=1,\ldots,17{,}541$; 7-day: $q_{\text{December 26,1949,January 1,1950},c}$, $c=1,\ldots,17{,}541$; 31-day: $q_{\text{December 2,1949,January 1,1950},c}$, $c=1,\ldots,17{,}541$

Using Hydrology Model to Build Resource Sheds

We built resource sheds by tracing input into each cell c (one at a time) over days $i,\ldots,j$ with the distributed hydrology model (DLBRM in our case) to find the tracer amounts at the location of interest (watershed mouth) for each day m, $m=i,\ldots,j$

$$q_{i,m,c}=\frac{\alpha_u\hat{U}^{i,m,c}_{m,M}+\alpha_\ell\hat{L}^{i,m,c}_{m,M}+\alpha_w\hat{G}^{i,m,c}_{m,M}+\alpha_s\hat{S}^{i,m,c}_{m,M}}{\alpha_u\hat{U}_{m,M}+\alpha_\ell\hat{L}_{m,M}+\alpha_w\hat{G}_{m,M}+\alpha_s\hat{S}_{m,M}},\quad m=i,\ldots,j$$
$$=\frac{\alpha_u\hat{U}^{i,j,c}_{m,M}+\alpha_\ell\hat{L}^{i,j,c}_{m,M}+\alpha_w\hat{G}^{i,j,c}_{m,M}+\alpha_s\hat{S}^{i,j,c}_{m,M}}{\alpha_u\hat{U}_{m,M}+\alpha_\ell\hat{L}_{m,M}+\alpha_w\hat{G}_{m,M}+\alpha_s\hat{S}_{m,M}},\quad m=i,\ldots,j \tag{27}$$

where $\hat{U}^{i,j,c}_{m,M}$=the upper soil zone storage tracer contents integrated over time interval m at cell M (the outlet cell) resulting from tracing cell c inputs over time intervals $i,\ldots,j$, $\hat{L}^{i,j,c}_{m,M}$, $\hat{G}^{i,j,c}_{m,M}$, and $\hat{S}^{i,j,c}_{m,M}$ are similarly defined for the lower soil zone, groundwater zone, and surface zone, and $\hat{U}_{m,M}$, $\hat{L}_{m,M}$, $\hat{G}_{m,M}$, and $\hat{S}_{m,M}$=upper soil, lower soil, groundwater, and surface zones total storage contents, respectively, integrated over time interval m at cell M (the outlet cell).

Fig. 7 shows example resource sheds for the Maumee River on January 1, 1950 from 1, 7, and 31 days of previous loading. In Fig. 7, the brightest areas correspond to cells contributing about 0.015% of the total flow on January 1, 1950. The darkest areas are close to zero. Note several things about Fig. 7. The southwestern and northwestern ridgelines are prominent as is a line to the north that marks the boundary between Ohio and Michigan (AB in Fig. 7). This boundary reflects the differences in the two states' definitions of some soil properties and so is an artifact of data standard differences. Point C in Fig. 7 identifies the mouth of the watershed. The first map in Fig. 7 shows a little response from the previous day's light rain near the mouth of the watershed. The second and third maps show most response along the edges of the watershed furthest from the mouth. Inspection of rainfall maps shows there is not much rainfall over the prior 4 days but there is a large amount 5 days prior in the southwest area. Also, spatially uniform rainfall fell over the entire watershed 7 days prior, 11–13 days prior, 15 days prior, 21 to 22 days prior, and 29 days prior. We can see the bright spot corresponding to the large peak

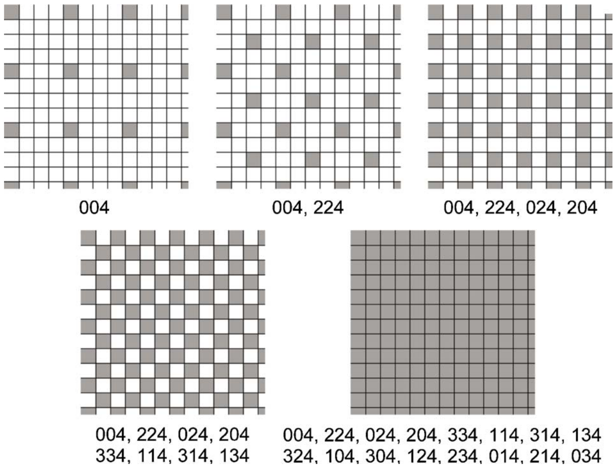

Fig. 8. Resource shed distribution map computation resolutions (digits indicate x offset, y offset, and spacing, respectively)

5 days earlier; the area closer to the mouth is relatively dark in the second and third maps because the only supplies there (7 or more days earlier) had already run off and are not part of the flow on this day. Note also that what happens prior to 7 days changes the picture very little (compare the last two maps). This is because the response of the watershed to supply is quick, on the order of 1–6 or 7 days, depending on location within the watershed. Most all supplies falling more than 6 or 7 days ago have already runoff and do not form a part of the flow on this day. The picture undoubtedly would be different for other materials, such as sediment, which reside along the flow paths temporarily, increasing the time it takes to reach the location of interest.

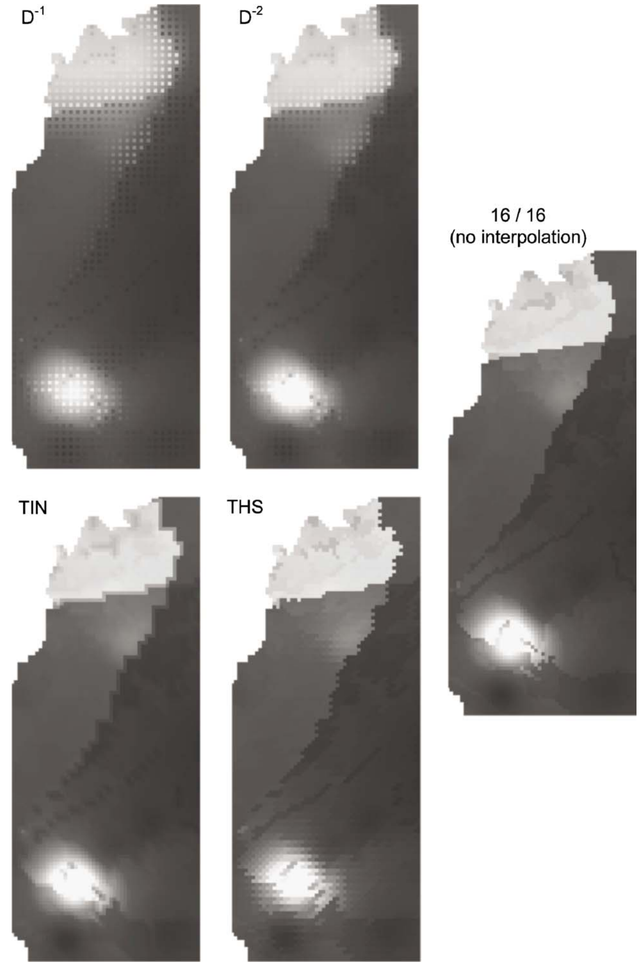

Fig. 9. Western Maumee resource shed distribution map interpolations and resolutions

Computation Reduction

Estimation, Interpolation, and Resolution

We can simulate for a sample of cells distributed uniformly over the watershed; see Fig. 8 in which the three-digit codes beneath each resolution example refer to horizontal and vertical offsets and spacing, respectively. We can interpolate between sampled cells to estimate values at the other cells. As computer resources become available, we can simulate separate samples of cells on different computer processors simultaneously and add them to the previous sample to increase resolution, reducing interpolation errors. Alternatively, we could simulate for all cells of the watershed at a coarser resolution. However, the disadvantage of that approach is that we would not be able to combine with another simulation to improve resolution; instead we would have to simulate for all cells of the watershed at a finer resolution. The third example in the upper right corner of Fig. 8 has every 4 of 16 cells computed, which is 1 of 4, which is used in Fig. 9 for interpolated values.

We considered several interpolation schemes, as shown in Fig. 9 for the western Maumee watershed and compared them to the full resolution picture (no interpolation) to assess which one(s) best represent the nonlinear (full resolution) resource shed. At all resolutions, the inverse distance (D^{-1}) and inverse distance squared (D^{-2}) interpolations produce artifacts at the scale of the resolution (which may be barely discernible at the scale used in Fig. 9). The inverse distance squared gives better definition to the features than the inverse distance at all resolutions. The triangular irregular network (TIN) with linear interpolation does not produce the artifacts of the two inverse distance methods and gives better definition to features in the watershed. It also gives the most detailed picture of the structure of the three methods at all resolutions. Finally, the Thiessen method appears probably the most aesthetically pleasing since the contrast is better at all resolutions, giving the illusion of more detail. It also paints a true picture of the resolution being used. However, it can be argued that even though the Thiessen interpolation appears crisper than the corresponding TINs, it may not represent the actual surface as well. That appears to be the case here: see the bright spot in the southwest section of the watershed; the first three interpolations appear to capture the "double tail" lying to the southeast of the bright spot, while the Thiessen does not (compare with the rightmost picture where all cells are present, and no interpolation is required). On the other hand, the northwest "head" of the bright spot seems best represented in the Thiessen picture. Such tradeoffs between model sampling and interpolation must be understood to make decisions about what to use with the chosen distributed hydrology model.

Tracing Considerations

There are 17,541 1-km^2 cells in the Maumee River watershed. The DLBRM requires 0.2–0.4 s on today's desktop computers to simulate 1 day's hydrology from all of these cells, for any loading pattern (Croley et al. 2007). With 17,541 loading patterns (one tracing each cell's contribution), a 1-day simulation of loadings requires 1 to 2 h of computation. For 1-, 2-, …, 31-day simulations ending on the same date there are 496 simulation days, which require 20–41 days of computation. However, we do not need to model all cells for each loading pattern. The DLBRM is built such that it allows isolation of individual flow paths from others; i.e., contaminants always go downstream and only along flow network paths. The DLBRM employs the same flow network on all four "levels" of the model (U, L, G, S). So, if we first model all cells to determine all flows and storages for all cells, then for each cell we can trace its input downstream by modeling only cells along the flow path. Since all boundary and initial conditions are known from our first simulation, and no tracers are present in the excluded cells, this is sufficient to determine a cell's effects on the location of interest. (For other models, other determinations will have to be made as to which cells are truly necessary to be modeled to trace each cell's contribution to the outflow.) The flow path length from any cell to the outlet for the Maumee watershed varies between 1 and 318 cells, with a median of 163 cells and an average of 168.7108 cells (instead of 17,541 cells) per trace. This reduces tracing time to $168.7108/17{,}541 \cong 1\%$ (1/100th). However, because of additional overheads the actual reduction is to about 1.7% (1/60th). Thus, a 1-day simulation requires 1 to 2 min of computation, and a 496-day simulation (for 1-, 2-, …, 31-day resource sheds) requires about 8–17 h of computation.

Ordering Computations

Computation reduction may also be achieved through computation ordering. Consider the calculation of a resource shed, $q_{i,j,c}$ for specific values of i and j for all c, $c=1,\ldots,s_{i,j}/a$. There are $j-i+1$ days to simulate. If we wanted all resource sheds, $i=j-30,\ldots,j$ for each j over a long time period, then for every prior period from 1 to 31 days and for 365.25 end dates in an average year, there are $496\times 365.25=181{,}164$ simulation days required per year. However, we could utilize more information from one simulation with the hydrology model. Consider that one simulation from day i to day j actually gives us (for all c) $q_{i,j,c}$, $q_{i,j-1,c}$, $q_{i,j-2,c},\ldots,$ $q_{i,i,c}$ [see Eq. (27)]. Therefore, $365.25\times 31=11{,}323$ simulation days per year gives the same information as above with only 6.25% of the effort [when we want all resource sheds (say 1 to 30 days prior) for each day (j) of a long period].

Finally, there is interest in resource shed calculations in near-real time to aid in detection of watershed source areas responsible for pollutant transport to receiving waters on an event basis. This would aid in the management of watershed runoff for limiting harmful algal blooms or in the closing of beaches in the receiving waters. It would also enable more effective land use management within a watershed. Consider a watershed application where it is deemed sufficient each day to estimate the 31 resource sheds corresponding to prior periods of 1–31 days. As already seen, this would require 496 simulation days each day by the first method outlined previously (or about 8–17 h of computation each day), which may be impractical in near-real time. The second method (outlined immediately above) does not save computation since one 31-day simulation yields 31 resource sheds all ending on different days; we would again require 496 simulation days to calculate the 31 resource sheds of different durations all ending on the same day.

However, by saving all internal model moisture and tracer storages at the end of the day from the model for each of the first 30 durations (1 day–30 day), the next day we could make a 1-day simulation (for the 1-day resource shed) and use the saved internal storages (from yesterday's 1-day through 30-day simulations) as initial conditions in 30 one-day simulations to calculate the 2-day through 31-day resource sheds, respectively. By again saving all internal storages at the end of the day, we could repeat for the next day and so forth. We need only compute 31 one-day simulations (31 simulation days or about 31–62 min of computation per day). There are several ways to reduce computations further: change the hydrological model cell size from 1 km^2 to 2×2 km (4 km^2) to reduce the computations to one-fourth of the 1 km^2 model, use the 1 km^2 model cell size but use less than full resolution and interpolate (e.g., reducing resolution by half and interpolating would reduce computations by half), and use multiple processors (e.g., a 10-processor computer would do one-tenth of the total computations on each processor in parallel, reducing computation times to one-tenth). Any or a combination of these methods could reduce computations or computation time; for example, using a 10-processor machine at half resolution and interpolating for 1-km^2 model cell size reduces computation time by 20. That comes to about 1.5–3 min of computation per day; considering 20 such watersheds at one time comes to about 30–60 min, which means that producing the 1–31-day near-real time resource sheds each day for all watersheds about Lake Erie is practical in near-real time. (We are currently linking Maumee resource sheds to Lake Erie resource sheds and are adding other watersheds as we finish calibrating them.)

Summary

A resource shed is defined as the area contributing material, over one time interval, passing through a location of interest over another time interval. We looked at definitions and concepts that preceded the resource shed concept and discussed interpretations in several fields. We also contrasted the concept with watersheds. Our focus was to present resource shed definitions and mathematics and to illustrate it for a simple material (water). Following this introduction, we provided rigorous general definitions of resource sheds and derived expressions for resource sheds where materials departing during one time interval arrive at the location of interest during a later time interval (definition 1), resource sheds where materials departing during a sequence of time intervals arrive at the location of interest during the last of those time intervals (definition 2), and resource sheds where materials departing during a sequence of time intervals arrive at the location of interest during that same sequence of time intervals (definition 3). We also expressed each of these resource sheds in terms of each other and showed that definition 2 resource sheds are contained in others with a longer departing time for the same arrival interval. Likewise, definition 3 resource sheds are contained in others with earlier start times and the same end times. These definitions of resource sheds as areas of source materials were illustrated with an example: the classical travel-time isochronal map for a watershed, used to build a watershed's time-area histogram for use in deriving a synthetic unit hydrograph.

We then provided rigorous general definitions of resource shed "distributions" and derived expressions for the distributed amount of source material within a resource shed, for all three definitions of the same. We again expressed each of the resource shed distributions in terms of each other and showed that resource shed distributions are contained by others with earlier start times, analogous to resource sheds themselves, for both definitions 2 and

3. We discussed the estimation of resource shed distributions (corresponding to all three definitions) within a watershed through the use of a spatially and vertically distributed hydrology model, in which the watershed area consists of discrete cells, by first defining resource shed distributions in terms of discrete space and showing their interrelationships with each other, presenting the distributions in terms of relative fractions of the material passing through the location of interest, introducing a specific example hydrology model for use on the Maumee River watershed in Ohio, and calculating example resource shed distributions of water for January 1, 1950 for three different periods of previous loadings.

The large amount of computation sometimes required in the construction of resource sheds and their distributions encourages methods to reduce calculations. We can calculate resource shed distributions over only a sample of watershed cells and then interpolate for the other cells. We explored alternate resolution trade-offs and a few spatial interpolation technique trade-offs. Tracing a material from a cell to the location of interest can occur, depending on the hydrology model, by simulating tracer movements only along the individual flow path from the cell to the location of interest, thus considerably reducing computation requirements. Also, we can order resource shed computations, when more than one resource shed is required, to save on computations. Ordering makes sense when contiguous dates and durations are considered or in near-real time where yesterday's computations are extended 1 day in today's.

It should be possible to extend this work in several ways. Currently, we are linking hydrological watershed resource sheds and their distributions with lake resource sheds generated via different methods (Croley et al. 2007). We plan to produce, for the World Wide Web, a dynamic linking of several Lake Erie watersheds with the lake to produce joint resource sheds and their distributions associated with about 35 locations of interest in the lake and extending into the tributary watersheds. Also, as we add material transport capabilities to our hydrology model, we will produce resource sheds and their distributions for sediment, nutrients, insecticides, and microbes that may be of more direct use in the prediction of harmful algal blooms and beach closings than simply water transport. Finally, in support of these latter predictions, we are also building a daily near-real time generator of resource sheds and their distributions; please see http://www.glerl.noaa.gov/res/Programs/pep/resourceshed/maps.php on the World Wide Web.

Acknowledgments

The writers thank Donna Kashian of the Great Lakes Environmental Research Laboratory (GLERL) and the three anonymous reviewers who helped us to increase the paper's clarity. This is GLERL contribution number 1,426 and is sponsored in part by New York Sea Grant award number R/CD-27 ("Great Lakes resource shed delineation"). Although reviewed by the USEPA and approved for publication, it may not necessarily reflect official agency policy.

Notation

The following symbols are used in this paper:

A_c = set of all locations comprising cell c;
a = area of A_c, $c=1,\ldots,v_{i,j}/a$ (all cells have the same area);
b = spatial distribution function used in calibration;
C = upper soil zone storage capacity (in Fig. 5);
C_c^U = observed upper soil zone available water capacity for the cth cell in a watershed;
c = watershed surface cell number;
e_p = potential evapotranspiration rate (in Fig. 5);
$f(\omega,a,b,c,d)$ = spatial density of material (mass/area) at location ω departing during $[a,b)$ and arriving at the location of interest (LOI) during $[c,d)$;
G = groundwater zone storage moisture (in Fig. 5);
$\hat{G}_{m,M}$ = groundwater zone total storage contents integrated over time interval m at cell M;
$\hat{G}_{m,M}^{i,j,c}$ = the groundwater zone storage tracer contents integrated over time interval m at cell M resulting from tracing input over time intervals $i,\ldots,j$ into cell c;
g = upstream lateral inflow into groundwater storage (in Fig. 5);
g_j = total material arriving at LOI in time interval j;
h = upstream lateral inflow into surface storage (in Fig. 5);
$h(\omega,\tau,t)$ = areal density rate of change with departure and arrival times of material (mass/area/time/time) departing location ω at time τ and arriving at LOI at time t;
K_c^U = observed upper soil zone permeability for the cth cell in a watershed;
L = lower soil zone storage moisture (in Fig. 5);
$\hat{L}_{m,M}$ = lower soil zone total storage contents integrated over time interval m at cell M;
$\hat{L}_{m,M}^{i,j,c}$ = the lower soil zone storage tracer contents integrated over time interval m at cell M resulting from tracing input over time intervals $i,\ldots,j$ into cell c;
ℓ = upstream lateral inflow into lower soil zone storage (in Fig. 5);
M = index of the cell corresponding to the outlet cell;
m = snow melt (in Fig. 5);
n = number of cells in the watershed;
$p_{i,j,c}$ = material fraction arriving at the LOI in time interval j that departed in time interval i from area A_c;
$q_{i,j,c}$ = material fraction arriving at the LOI in time interval j that departed during time intervals $i,\ldots,j$ from area A_c;
$R(a,b,c,d)$ = set of all locations (resource shed) where materials departing during time interval $[a,b)$ arrive at the LOI during time interval $[c,d)$;
S = surface storage moisture (in Fig. 5);
$S_{i,j}$ = set of all locations (resource shed) where materials departing during time intervals $i,\ldots,j$ arrive at the LOI during time interval j;
$\hat{S}_{m,M}$ = surface zone total storage contents integrated over time interval m at cell M;

$\hat{S}^{i,j,c}_{m,M}$ = the surface zone storage tracer contents integrated over time interval m at cell M resulting from tracing input over time intervals $i,\ldots,j$ into cell c;

s = water supply to watershed surface (in Fig. 5);

$s_{i,j}$ = area of $S_{i,j}$;

T_b = potential evapotranspiration base temperature (in Fig. 5);

$T_{i,j}$ = set of all locations (resource shed) where materials departing during time intervals $i,\ldots,j$ arrive at the LOI also during time intervals $i,\ldots,j$;

t = time;

$t_{i,j}$ = area of $T_{i,j}$;

U = upper soil zone storage moisture (in Fig. 5);

$\hat{U}_{m,M}$ = upper soil total storage contents integrated over time interval m at cell M;

$\hat{U}^{i,j,c}_{m,M}$ = the upper soil zone storage tracer contents integrated over time interval m at cell M resulting from tracing input over time intervals $i,\ldots,j$ into cell c;

u = upstream lateral inflow into upper soil zone storage (in Fig. 5);

$u_{i,j,c}$ = material fraction arriving at the LOI during time intervals $i,\ldots,j$ that departed during time intervals $i,\ldots,j$ from area A_c;

$V_{i,j}$ = set of all locations (resource shed) where materials departing during time interval i arrive at the LOI during time interval j;

$v_{i,j}$ = area of $V_{i,j}$;

$w_{i,j}(\omega)$ = areal density of material at location ω departing during time intervals $i,\ldots,j$ and arriving at the LOI also during time intervals $i,\ldots,j$;

$\bar{w}_{i,j,c}$ = mass of material in watershed surface cell c departing during time intervals $i,\ldots,j$ and arriving at the LOI also during time intervals $i,\ldots,j$;

$x_{i,j}(\omega)$ = areal density of material at location ω departing during time interval i and arriving at the LOI during time interval j;

$\bar{x}_{i,j,c}$ = mass of material in watershed surface cell c departing during time interval i and arriving at the LOI during time interval j;

$Y(\tau,t)$ = set of all locations where materials departing at time τ arrive at the LOI at time t;

y_c = observed data value for cell c;

$z_{i,j}(\omega)$ = areal density of material at location ω departing during time intervals $i,\ldots,j$ and arriving at the LOI during time interval j;

$\bar{z}_{i,j,c}$ = mass of material in watershed surface cell c departing during time intervals $i,\ldots,j$ and arriving at the LOI during time interval j;

α_d = deep percolation linear reservoir coefficient (in Fig. 5);

α_g = groundwater linear reservoir coefficient (in Fig. 5);

α_i = interflow linear reservoir coefficient (in Fig. 5);

α_ℓ = linear reservoir coefficient for downstream lateral outflow from lower soil zone storage (in Fig. 5);

α_m = degree-day coefficient for snow melt (in Fig. 5);

α_p = percolation linear reservoir coefficient (in Fig. 5);

α_s = cell outflow linear reservoir coefficient (in Fig. 5);

α_t = potential evapotranspiration heat balance coefficient (in Fig. 5);

α_u = linear reservoir coefficient for downstream lateral outflow from upper soil zone storage (in Fig. 5);

α_w = linear reservoir coefficient for downstream lateral outflow from groundwater storage (in Fig. 5);

β_g = partial linear reservoir coefficient for evapotranspiration from groundwater storage (in Fig. 5);

β_ℓ = partial linear reservoir coefficient for evapotranspiration from lower soil zone storage (in Fig. 5);

β_s = partial linear reservoir coefficient for evapotranspiration from surface storage (in Fig. 5);

β_u = partial linear reservoir coefficient for evapotranspiration from upper soil zone storage (in Fig. 5);

$\gamma_{i,j,m}$ = fraction of all material arriving at the LOI during time intervals $i,\ldots,j$ that arrived in time interval m;

δ = length of time interval used in discrete-time resource shed definitions; i.e., time interval i is $[i-\delta, i)$;

ε = fraction of observed range (in percent) used as parameter range;

τ = time;

$\forall$ = denotation of range; e.g., $\forall\ \omega \in A$, denotes for all ω within set A;

$\cup$ = operator representing union of sets;

$\varnothing$ = the empty set;

$\subset$ = denotation of inclusion; i.e., $A \subset B$ denotes set A is contained in set B;

$\in$ = denotation of inclusion; e.g., $\forall\ \omega \in A$, denotes for all ω within set A; and

$\Rightarrow$ = denotation of implication; e.g., "$A \subset B$ and $B \subset C \Rightarrow A \subset C$" denotes "set A is contained in B and B is contained in C implies A is contained in C."

References

Bagtzoglou, A. C., and Atmadja, J. (2005). "Mathematical methods for hydrologic inversion: The case of pollution source identification." *Environmental impact assessment of recycled wastes on surface and ground waters: Chemodynamics, toxicology, and modeling. the handbook of environmental chemistry, water pollution series*, Vol. 5, Part F, Springer, Berlin–Heidelberg, 739–770.

Ben-David, M., Blundell, G. M., Kern, J. W., Maier, J. A. K., Brown, E. D., and Jewett, S. C. (2005). "Communication in river otters: Creation of variable resource sheds for terrestrial communities." *Ecology*,

86(5), 1331.
Brunckhorst, D., and Reeve, I. (2006). "A geography of place: Principles and application of defining 'eco-civic' resource governance regions." *Austral. Geograph.*, 37(2), 147–166.
Chang, M., and Cardelino, C. (2000). "Application of the urban airshed model to forecasting next-day peak ozone concentrations in Atlanta." *J. Air Waste Manage. Assoc.*, 50(11), 2010–2024.
Chemical Rubber Company (CRC). (1969), "Calculus, integrals, elementary forms." *Standard mathematical tables*, S. M. Shelby, ed., 17th Ed., The Chemical Rubber Company, Cleveland, Ohio, 404.
Chow, V. T., Maidment, D. R., and Mays, L. W. (1988). *Applied hydrology*, McGraw-Hill, New York.
Cousins, S. H. (1990). "Countable ecosystems deriving from a new food web entity." *Oikos*, 57(2), 270C–275C.
Croley, T. E., II. (2002). "Large basin runoff model." *Mathematical models in watershed hydrology*, V. Singh, D. Frevert, and S. Meyer, eds., Water Resources, Littleton, Colo., 717–770.
Croley, T. E., II, and He., C. (2005). "Distributed-parameter large basin runoff model. I: Model development." *J. Hydrol. Eng.*, 10(3), 173–181.
Croley, T. E., II, and He., C. (2006). "A watershed surface and subsurface spatial intraflows model." *J. Hydrol. Eng.*, 11(10), 12–20.
Croley, T. E., II, He., C., Atkinson, J. F., and Raikow, D. F. (2007). "Resource shed definitions and computations." *NOAA Tech. Memo. GLERL-141*, Great Lakes Environmental Research Laboratory, Ann Arbor, Mich., 43 pp.
Croley, T. E., II, He, C., and Lee, D. H. (2005). "Distributed-parameter large basin runoff model. II: Application." *J. Hydrol. Eng.*, 10(3), 182–191.
Ellis, A. W., Brommer, D. M., and Balling, R. C. (2006). "Climatic conditions linked to high PM10 concentration in a bi-national airshed: Nogales (Arizona, USA, and Sonora, Mexico)." *Clim. Res.*, 30(2), 113–124.
Habermacher, F. D., Napelenok, S. L., Akhtar, F., Hu, Y., and Russell, A. G. (2007). "Area of influence (AOI) development: Fast generation of receptor-oriented sensitivity fields for use in regional air quality modeling." *Environ. Sci. Technol.*, 41(11), 3997–4003.
He, C., Cheng, S., and Luo, Y. (2005). "Desiccation of the Yellow River and the South Water Northward Diversion Project." *Water Int.*, 30(2), 261–268.
Kalin, L., Govindaraju, R. S., and Hantush, M. M. (2004). "Development and application of a methodology for sediment source identification. I: Modified unit sedimentograph approach." *J. Hydrol. Eng.*, 9(3), 184–193.
Linsley, R. K., Jr., Kohler, M. A., and Paulhus, J. L. H. (1982). *Hydrology for engineers*, 3rd Ed., McGraw-Hill, New York, 508 pp.
Mast, M. A., Foreman, W. T., and Skaates, S. V. (2007). "Current-use pesticides and organochlorine compounds in precipitation and lake sediment from two high-elevation national parks in the western United States." *Arch. Environ. Contam. Toxicol.*, 52(3), 294–305.
Michel, S. M. (2000). "Defining hydrocommons governance along the border of the Californias: A case study of transbasin diversions and water quality in the Tijuana-San Diego metropolitan region." *Nat. Resour. J.*, 40(4), 931–972.
Morawska, L., Vishvakarman, D., Mengersen, K., and Thomas, S. (2002). "Spatial variation of airborne pollutant concentrations in Brisbane, Australia and its potential impact on population exposure assessment." *Atmos. Environ.*, 36(21), 3545–3555.
Murphy, B. L. and Morrison, R. D. (2007). *Introduction to environmental forensics*, 2nd Ed., Elsevier Academic, Burlington, Mass.
National Research Council. (1999). *New strategies for America's watersheds*, National Academy Press, Washington, D.C.
Oswood, M. W., Reynolds, J. B., Irons, J. G., and Milner, A. M. (2000). "Distribution of freshwater fishes in ecoregions and hydroregions of Alaska." *J. North Am. Benthol. Soc.*, 19(3), 405–418.
Polis, G. A., Anderson, W. A. and Holt, R. D. (1997). "Toward an integration of landscape and food web ecology." *Annu. Rev. Ecol. Syst.*, 28, 289–316.
Power, M. E., and Rainey, W. E. (2000). "Food webs and resource sheds: Towards spatially delimiting trophic interactions." M. J. Hutchings, E. A. John, and A. J. A. Stewart, eds., *The ecological consequences of environmental heterogeneity*, Blackwell Science, Oxford, U.K., 291–314.
Santoul, F., Soulard, A., Figuerola, J., Crghino, R., and Mastrorillo, S. (2004). "Environmental factors influencing local fish species richness and differences between hydroregions in south-western France." *Int. Rev. Hydrobiol.*, 89(1), 79–87.
Tullar, I. V., and Suffet, I. H. (1975). "Fate of vanadium in an urban airshed-lower Delaware River Valley." *J. Air Pollut. Control Assoc.*, 25(3), 282–286.
U.S. Environmental Protection Agency (USEPA). (1995). "Watershed protection: A statewide approach." *Rep. No. EPA 841-R-95-004*. Office of Water, Washington, D.C.
U.S. Geological Survey (USGS). (2001). "Approach for delineation of contributing areas and zones of transport to selected public-supply wells using a regional ground-water flow model, Palm Beach County, Florida." R. A. Renhen, R. D. Patterson, L. L. Orzol, and J. Dixon, eds., U.S. Geological Survey, *Water-Resources Investigations Report 01-4158*.